

More than simply Iron: Macro- to Microscopic Cellular Iron Distribution in the Brain Determines MR Contrast

Evgeniya Kirilina^{1,2}, Markus Morawski³, Katja Reimann³, Isabel Weigelt³, Steffen Jankuhn⁴, Larissa Müller⁵, Norbert Jakubowski⁵ and Nikolaus Weiskopf¹

¹ Department of Neurophysics, Max Planck Institute for Human Cognitive and Brain Sciences, Leipzig, Germany

² Center for Computational Neuroscience Berlin, Free University Berlin, Germany

³ Paul-Flechsig-Institute for Brain Research, Leipzig University, Germany

⁴ Department of Solid State Physics, Faculty of Physics and Earth Sciences, Leipzig University, Germany

⁵ Federal Institute for Materials Research and Testing, Berlin, Germany



MAX-PLANCK-GESELLSCHAFT

MAX
PLANCK
INSTITUTE
FOR
HUMAN
COGNITIVE AND BRAIN SCIENCES
LEIPZIG

Introduction

Next to myelin iron is the other major source of MR contrast in the brain. It dominates $R2^*$, $R2$ and QSM cortical profiles, MR-contrast in subcortical areas and contributes to white matter contrast. Aiming at methodological breakthroughs like in-vivo Brodmann mapping or MR-based iron quantification, significant theoretical and experimental efforts were devoted to the understanding of iron-induced MR-contrast. Different to the case of myelin, where the relationship between tissue microstructure and MR parameters is widely accepted, the impact of the cellular and subcellular iron distribution is much less explored. Therefore, usually a single set of linear coefficients is employed to relate tissue iron concentration and quantitative MR parameter maps. A major reason for this simplification is a lack of quantitative knowledge on the cellular and subcellular iron distribution. Beyond this, the interplay between the microscopic iron distribution and diffusion in creating MR contrast is not fully understood. Herein, we close this gap by combining state of the art quantitative 7T MRI with cutting edge quantitative iron and myelin mapping on post mortem brain samples.

Methods

Post-mortem MRI

Post-mortem human brain blocks (male, 78 years, post-mortem time before fixation 16h, temporal lobe, female, 71 years, post-mortem time before fixation 26h, midbrain) were obtained from the Neuropathology Department of Leipzig University, Germany. $R1$ maps (isotropic resolution of 0.23mm) were obtained using the MP2RAGE, $R2^*$ maps and QSMs (isotropic resolution of 0.21mm and 0.06mm) using multi-echo FLASH sequences. QSMs were reconstructed using the HEIDI algorithm (Schweser et al. 2012). Quantitative $R2$ maps of a single slice were obtained using TSE sequence in plane resolution 0.21x0.21mm² and multiple TEs.

Tissue de-ironing

One subsample (temporal lobe) was subjected to a de-ironing procedure. It was incubated in a solution of 2% desferal and 2% sodiumdithionite solved in PBS at 37°C for a period of 15 days to remove the iron in the tissue.

Quantitative Iron Microscopy: Proton Induced X-Ray Emission (PIXE)

Quantitative elemental maps with microscopic resolution were obtained by PIXE, using the high-energy ion nano-probe LIPSION at the Leipzig University. LIPSION provides a 1μm proton beam of 2,25MeV energy. The proton beam was scanned over multiple 200x200μm² and 400x400 μm² seized brain sections, while the induced X-rays emitted from the sample were recorded. From the recorded X-rays, quantitative iron maps were created using GeoPIXE software. Resulting maps were smoothed with a Gaussian filter, with 2μm kernel.

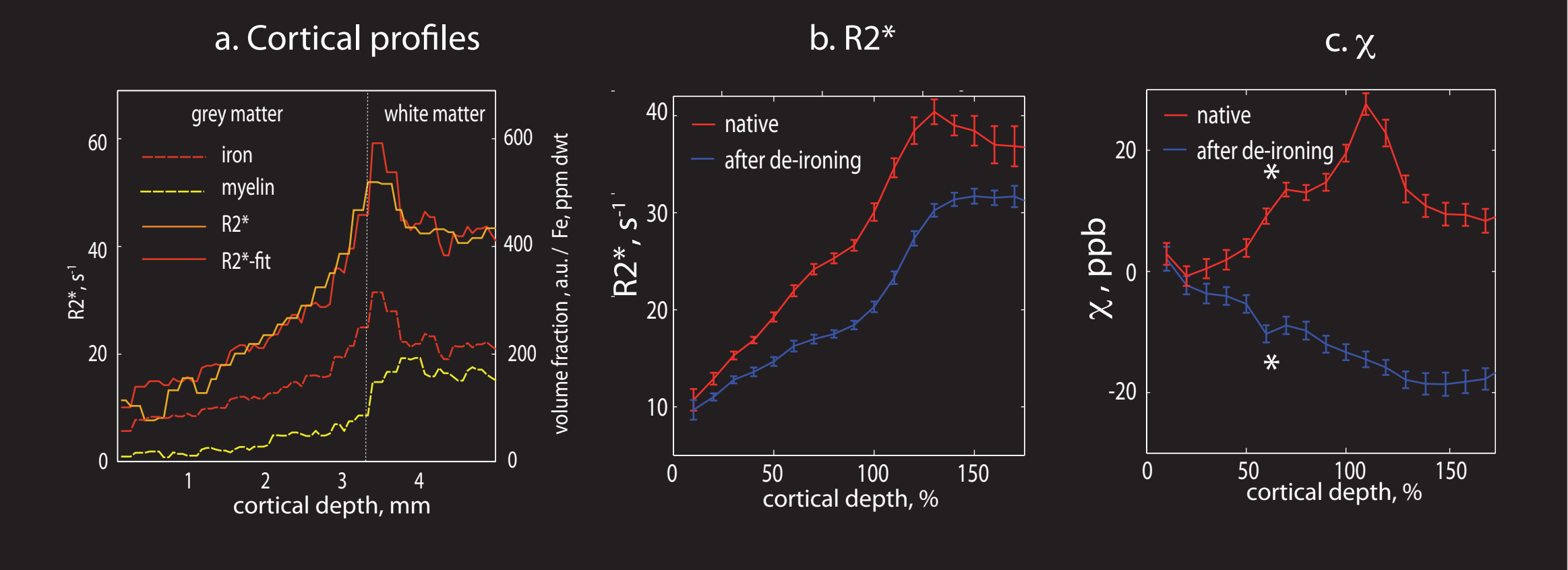
Quantitative Iron Mapping: Laser Ablation Inductively Coupled Mass Spectroscopy (LA ICP MSI)

Quantitative elemental maps were obtained using Laser Ablation (LA) system (NWR213, ESI, Portland, USA) combined with inductively coupled plasma (ICP) sector field mass spectrometer (Element XR, Thermo Fisher Scientific, Germany). This setup provided quantitative elemental maps with in-plane resolution of 120x61μm². The isotopes ³¹P, ³⁴S and ⁵⁷Fe were selected for analysis. Myelin volume fraction maps were calculated from P and S maps (Stüber et al., 2014).

Results

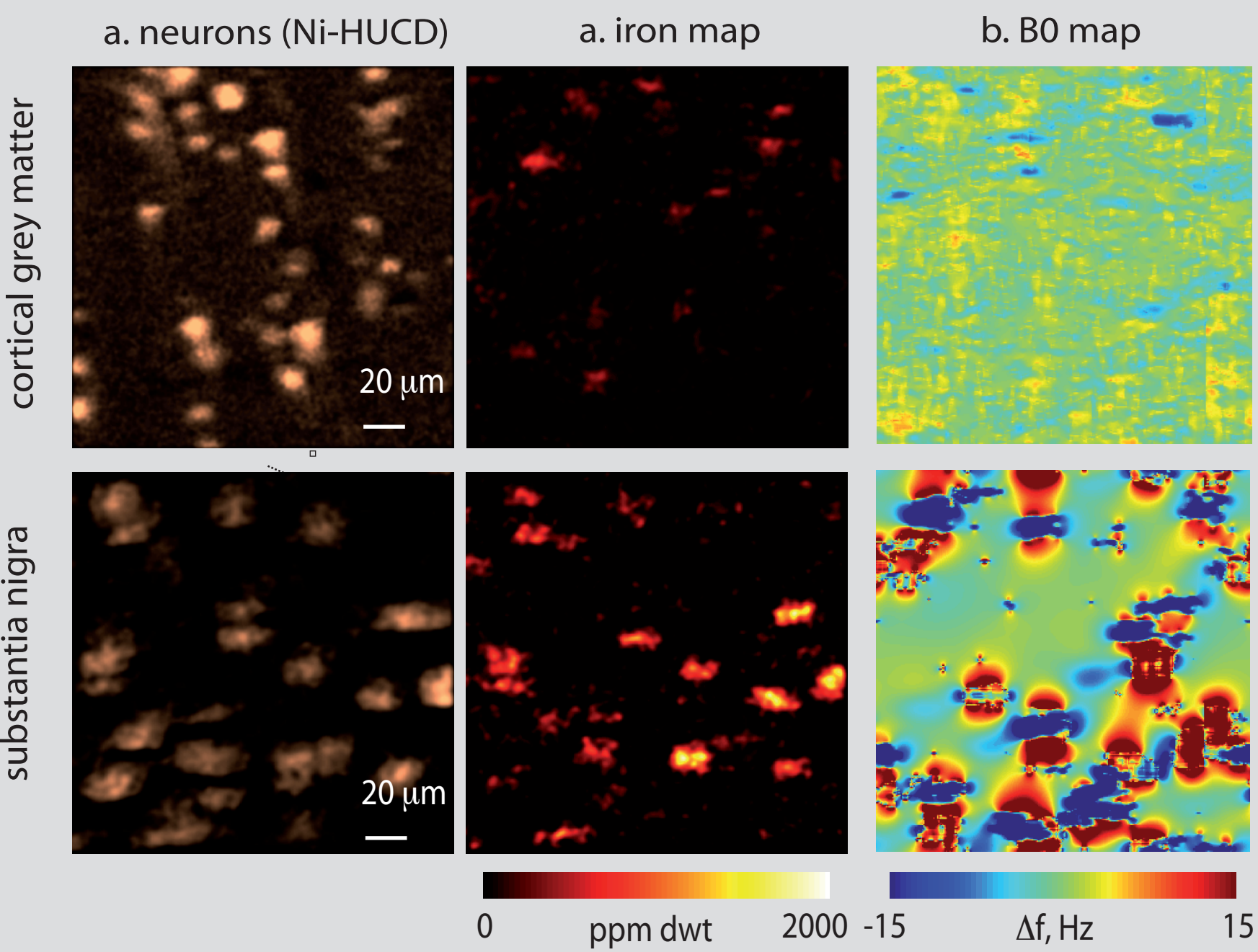
Grey Matter

Iron concentration increases with cortical depth and determines cortical profiles of $R2^*$ and χ



(a) Cortical profiles of $R2^*$, iron concentration and myelin volume fraction obtained with LA ICP MSI. Iron and myelin concentrations increase with cortical depth. Elevated level of iron was observed in a thin (0.5 mm) stripe in subcortical white matter. Cortical profiles of $R2^*$ can be well fitted by a linear combination of myelin and iron contributions. Impact of iron on $R2^*$ (b) and χ (c) can be seen on the changes of these parameters upon iron removal. Note inversion of QSM contrast for fiber-rich cortical layer IV.

Cellular distribution of iron influences MR line shape

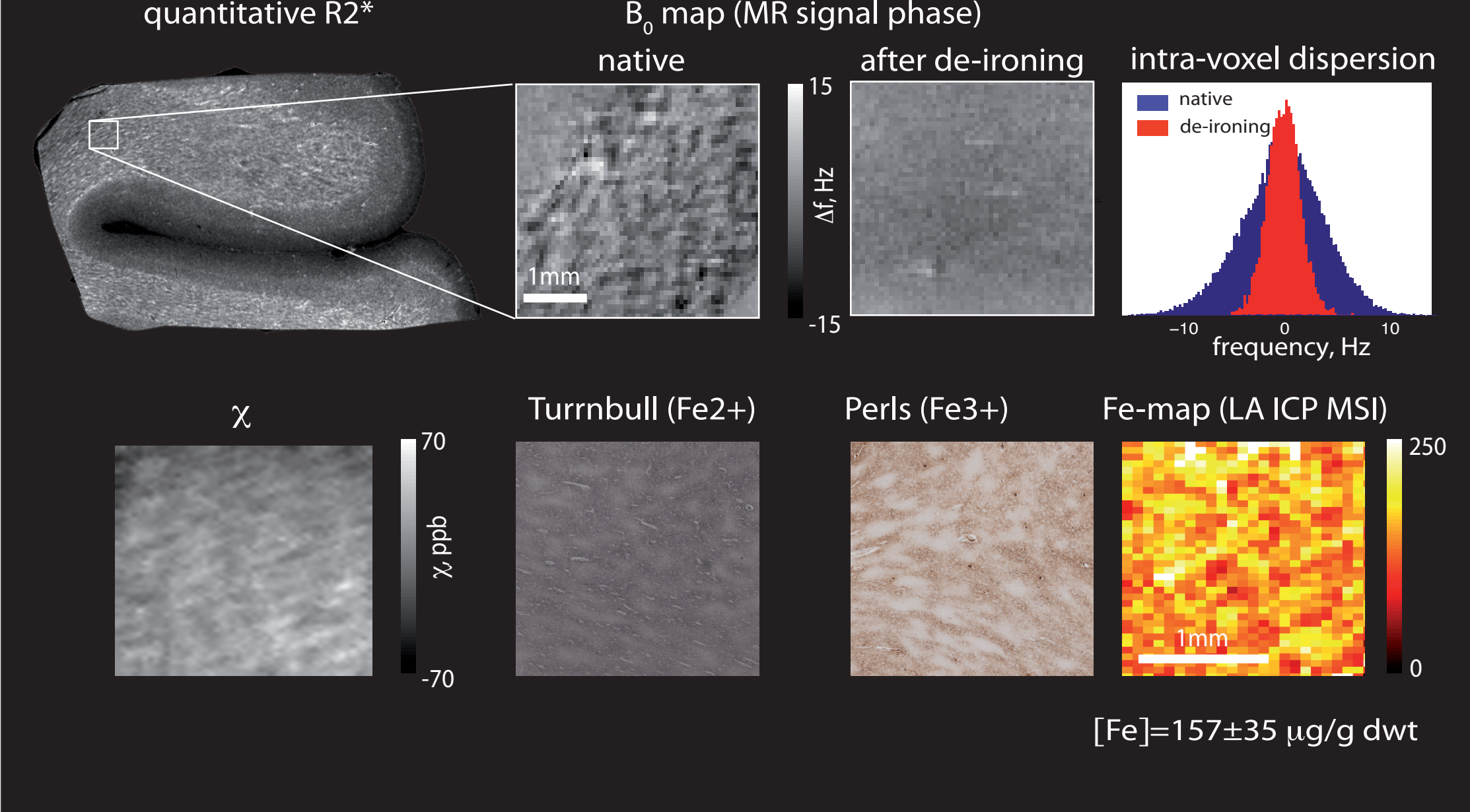


In cortical grey matter iron hotspots are localized in sparsely-distributed oligodendrocytes and astroglia. Neurons are iron-poor.

In substantia nigra densely packed iron-rich neurons contain most of the iron and dominate MR-contrast.

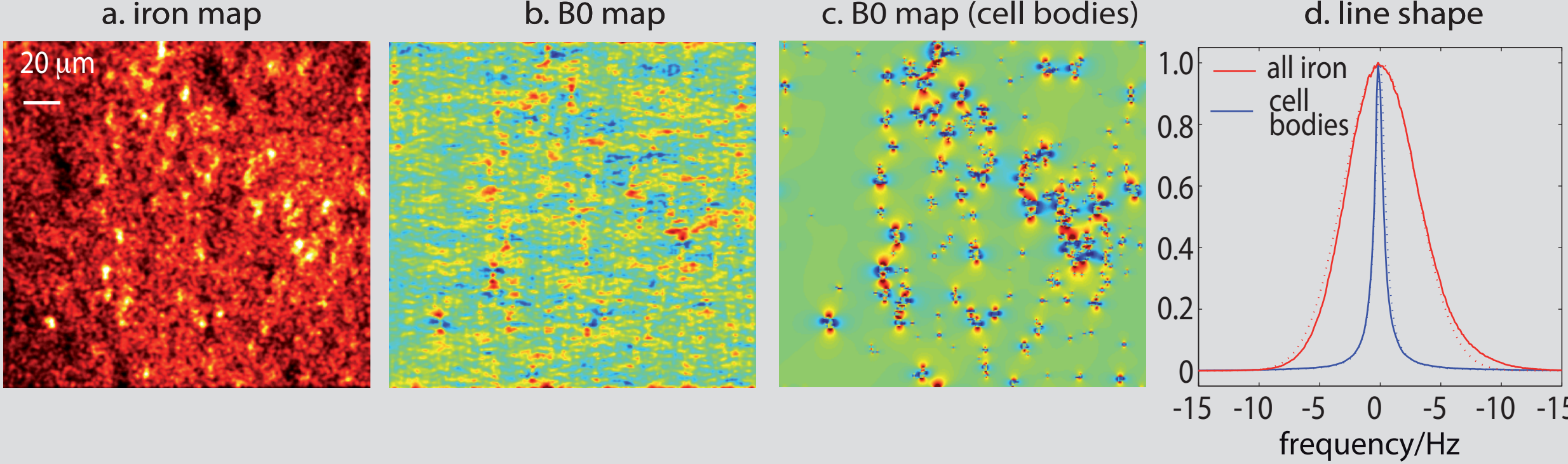
White Matter

Iron-rich patches around small vessels in white matter contribute to $R2^*$ and χ



Iron in white matter appears in patches with characteristic size of 100-200 μm. The patches are observed in classical Perl's and Turnbull's iron stains as well as in quantitative iron maps obtained with LA ICP MSI. They induce substantial (8 Hz) intra-voxel de-phasing when resolution lower than 0.2 mm is used and therefore contribute to $R2^*$ in white matter.

$R2^*$ contrast in SWM is driven by iron in oligodendrocytes and fibers



(a) PIXE iron maps in subcortical white matter show iron hotspots in the somas of oligodendrocytes (size of 5 μm) which contain up to 10 % of overall iron. The high iron background levels may either originate from iron rich fibers or iron rich oligodendrocyte processes. (b) Simulated map of microscopic distortion of magnetic field B_0 resulting from iron distribution. (c) Simulated map of $B0$ distribution resulting only from the iron-rich oligodendrocyte bodies. (d) MR line shape resulting from magnetic field distribution (b) and (c) overlaid with fit using Gaussian and Lorentzian line shapes respectively. Note that Gaussian line broadening resulting from iron-rich fibers dominates in white matter.

Macro- to Mesoscopic Scales

Micorscopic Scales

Conclusions

Iron is inhomogenously distributed in both grey and white matter. Furthermore, different scales of inhomogeneity determine the MR contrast in the different compartments. In grey matter iron rich fibers, and small (1-3μm) micro-, astro- and oligodendroglia contained most of the iron and were sparsely distributed. In superficial and deep white matter, however, oligodendrocytes somas with the sizes of 5±1.5μm (distance between cells of 20±5μm) and iron rich fibers contained most of the iron. Iron in cell bodies result in Lorentzian line broadening, while iron-rich fibers induces Gaussian line broadening and dominates in white matter.

In addition, patches of enhanced iron concentration around small vessels with a typical size of 100-200μm contribute 10-20% of $R2^*$ and QSM a in white matter. A different contrast mechanism prevailed in brain nuclei where densely packed 20μm large iron loaded neurons dominated the MR contrast. These results provide an important basis for understanding the iron induced MR-contrast and its microstructural underpinnings. Based on these measured microscopic iron distributions and a Gaussian diffusion model we are now in the process of simulating the MR contrast mechanisms in different tissue types.